We are IntechOpen, the world's leading publisher of Open Access books Built by scientists, for scientists

4,800
Open access books available

122,000
International authors and editors

135M
Downloads

Our authors are among the

154
Countries delivered to

TOP 1%
most cited scientists

12.2%
Contributors from top 500 universities

CLARIVATE ANALYTICS BOOK CITATION INDEX INDEXED

WEB OF SCIENCE™

Selection of our books indexed in the Book Citation Index in Web of Science™ Core Collection (BKCI)

Interested in publishing with us?
Contact book.department@intechopen.com

Numbers displayed above are based on latest data collected.
For more information visit www.intechopen.com

Chapter 3

Classification of Mass-Produced Carbon Nanotubes and Their Physico-Chemical Properties

Heon Sang Lee

Additional information is available at the end of the chapter

http://dx.doi.org/10.5772/52613

1. Introduction

Carbon nanotube (CNT) may be classified into single walled (SWCNT), double walled (DWCNT), and multiwalled carbon nanotube (MWCNT) according to the number of graphene layers. In some cases, bamboo-shaped multiwalled carbon nanotubes were also synthesized. Among these carbon nanotubes, multiwalled carbon nanotubes have been mass-produced in hundreds metric tons level. Many researchs on multiwalled carbon nanotubes point to an electrode, polymer composites, coating, and others. The number of graphene layers, purity, and crystallinity are the main features of multiwalled carbon nanotubes, which need to be characterized. We have proposed one important characteristic of multiwalled carbon nanotubes, the mesoscopic shape of MWCNT, of which many industrial applications may be comprised. According to our suggestion, one can determine the degree of tortuousness of MWCNT, quantitatively. (*see ref.1-5 and sections 1-6 in this chapter*)In this chapter, we will describe the mesoscopic shape factor of MWCNT in detail. Various physical properties as well as toxicity may strongly depend on the mesoscopic shape factor of MWCNT. Our suggestion has also been published as an international standard ISO/TS11888 by international organization for standardization (ISO) in 2011.

I hope readers enjoy the concepts and expressions shown in this chapter. Especially, this chapter shall be helpful to whom may want to develop a commercial application by selecting a proper CNT.

2. Static bending persistence length (SBPL, l_{sp})

If MWCNTs have no defect along their axis, their appearance would be straight to several hundred micro meter. Persistence length is the maximum straight length that is not bent by thermal energy. The persistence length of MWCNT is expected to be several hundred micro meter due to its exceptional high modulus. Static bending persistence length (SBPL) has been proposed in our earlier work to quantify the mesoscopic shape of MWCNT. SBPL is the maximum straight length that is not bent by permanent deformation. Fig. 1 shows the concept of SBPL. When a length considered is longer than SBPL, the shape of MWCNT looks tortuous. On the contrary, the shape of MWCNT looks straight as a length considered is shorter than SBPL.

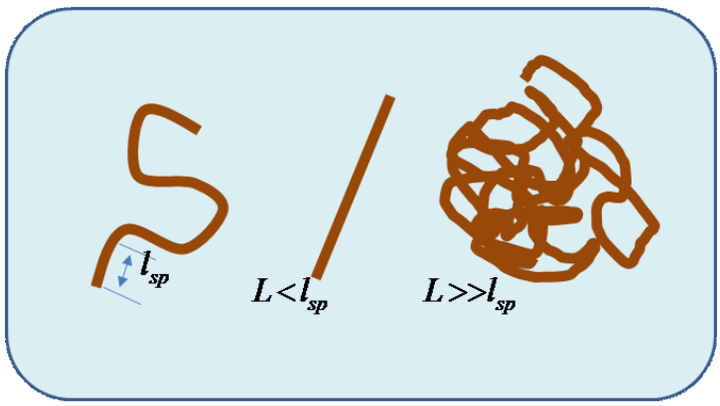

Figure 1. The concept of static bending persistence length of MWCNT (l_{sp}).

If length considered is longer than SBPL, the shape of MWCNT looks tortuous. On the contrary, the shape of MWCNT looks straight as a length considered is shorter than SBPL.

3. Mathematical expression of SBPL (l_{sp})

The end-to-end vector can be obtained such as eq 1 when the distribution of bending points ($\{\varphi\} \equiv (\varphi_1, \varphi_2, \ldots, \varphi_k)$) is given.

$$\mathbf{R} = N\sum_{i=1}^{k} \varphi_i \mathbf{r}_i \tag{1}$$

The spatial average of end-to-end distance $\langle \boldsymbol{R} \rangle$ should be zero, since probability to bend to one direction is the same as that to the opposite direction. Then spatial average of square end-to-end vector is obtained as eq 2

http://dx.doi.org/10.5772/52613

$$\left\langle \mathbf{R^2} \right\rangle = N^2 \sum_{i=1}^{k} \sum_{j=1}^{k} \left(\varphi_i \mathbf{r_i} \right) \cdot \left(\varphi_j \mathbf{r_j} \right) = N^2 b^2 D_b \tag{2}$$

$$D_b \equiv \left\langle \mathbf{R}^2 \right\rangle / L^2 \cong \sum_{i=1}^{k} \varphi_i^2 \tag{3}$$

where D_b is a bending ratio, $\varphi_i = N_i / N$, N_i is the number of unit segment in i-direction segment, N is the total number of unit segment, $k = m + 1$, m is the number of static bending points on a coil, and r_i is i-direction segment vector with the length of b. The expression shown in eq 3 is significant. This indicates that we can obtain the distribution function when we have enough data. This is often called as ill-posed problem. Regularization method in applied mathematics gives us the solution for solving the problems. Equation 3 holds only if a probability of the fold-back conformation is the same as that of the straight conformation.By using the scaling law, the coil expressed in eq 2 and 3 can be renormalized into the coil that has constant segment length, $2l_{p0}$. Then we can obtain eq 3 with $\varphi_i = 2l_{p0} / L$ and $k = L / 2l_{p0}$. We can also consider a case where the bent angle (θ) between the *ith* and *(i+1)*th segments is a fixed small angle. The spatial average of the square end-to-end vector is obtained as following

$$\left\langle \mathbf{r}_n \cdot \mathbf{r}_m \right\rangle = N \left(\sum_{i=1}^{k} \varphi_i^2 \right) b^2 \left(\cos\theta \right)^{|n-m|} \tag{4}$$

$$\left\langle \mathbf{R}^2 \right\rangle = \sum_{n=1}^{k} \sum_{m=1}^{k} \left\langle \mathbf{r}_n \cdot \mathbf{r}_m \right\rangle = \sum_{n=1}^{k} \sum_{p=-n+1}^{k-n} \left\langle \mathbf{r}_n \cdot \mathbf{r}_{n+p} \right\rangle \cong \sum_{n=1}^{k} \sum_{p=-\infty}^{\infty} \left\langle \mathbf{r}_n \cdot \mathbf{r}_{n+p} \right\rangle \tag{5}$$

$$\sum_{p=-\infty}^{\infty} \left\langle \mathbf{r}_n \cdot \mathbf{r}_{n+p} \right\rangle = N \left(\sum_{i=1}^{k} \varphi_i^2 \right) b^2 \left(1 + 2 \sum_{p=1}^{\infty} \cos^p \theta \right) = N \left(\sum_{i=1}^{k} \varphi_i^2 \right) b^2 \left(\frac{1+\cos\theta}{1-\cos\theta} \right) \tag{6}$$

$$\left\langle \mathbf{R}^2 \right\rangle = (N^2 b^2)(\sum_{i=1}^{k} \phi_i^2)(\frac{1+\cos(\theta)}{1-\cos(\theta)}) = L^2 D_b \tag{7}$$

$$D_b \equiv \frac{\left\langle \mathbf{R}^2 \right\rangle}{L^2} \cong \left(\sum_{i=1}^{k} \varphi_i^2 \right) \left(\frac{1+\cos\left(\theta\right)}{1-\cos\left(\theta\right)} \right) \tag{8}$$

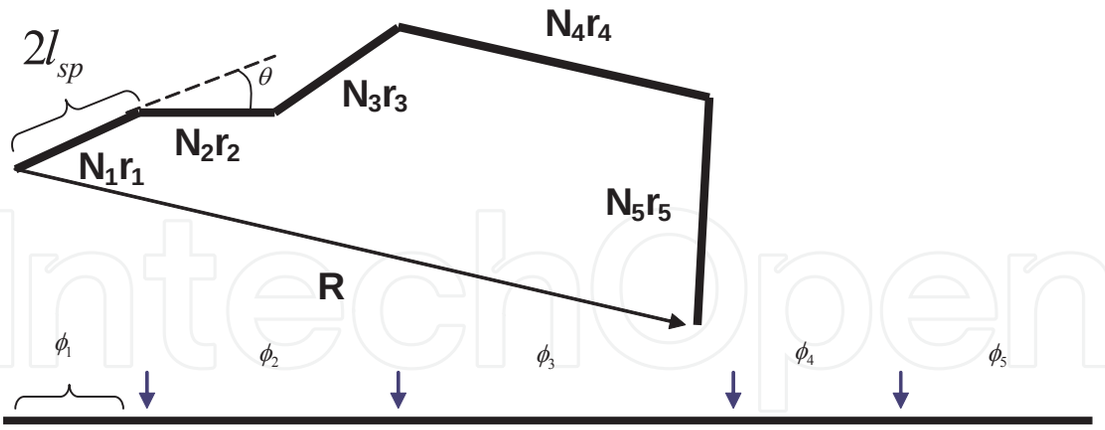

Figure 2. Tortuous MWCNT; bent points are distributed randomly along MWCNT axis.

Equation 7 can also be renormalized into the coil that has a constant segment length, $2l_{sp}$. The bending ratio (D_b) is expressed as eq 9

$$D_b \equiv \frac{\left\langle \mathbf{R}^2 \right\rangle}{L^2} \cong \left(\frac{2l_{p0}}{L} \right) \left(\frac{1+\cos(\theta)}{1-\cos(\theta)} \right) = C \left(\frac{2l_{p0}}{L} \right) = \frac{2l_{sp}}{L} \tag{9}$$

where $l_{sp}=Cl_{p0}$ is the static bending persistence length and Cshould be a constant for a fixed bent angle. The static bending persistence length is a statistical quantity, representing the maximum straight length that is not bent by static bending. In the case of continuous curvature, a more accurate statement is that the static bending persistence length is the mean radius of curvature of the rigid random-coil due to static bending. The same quantity arising from dynamic bending instead of static bending is dynamic bending persistence length (l_p). The dynamic bending persistence length represents the stiffness of the molecules as determined by the effective bending modulus against thermal energy in Brownian motion. Equation 5 is valid when $L >> l_{sp}$, the coil limit. $D_b=\langle \boldsymbol{R}^2 \rangle / L^2=1$ when $L < l_{sp}$, the rod limit.If we know the values of end-to-end distance and contour length, the bending ratio can be obtained from the mean-squared end-to-end distance divided by the mean-squared contour length. The end-to-end distance of RRC varies with the change of bending angle. The difference can be compromised by using an arbitrary unit segment length which is similar to the scaling of polymer chain. The mean-squared end-to-end distance by the Kratky-Porod (KP) expression is given by eq 10 when the dynamic bending persistence length (l_p) is replaced by the static bending persistence length (l_{sp}) and the twice l_{sp} equals to Kuhn length.

$$\left\langle \mathbf{R}^2 \right\rangle = 2l_{sp}L + 2l_{sp}^2 \left(e^{-L/l_{sp}} - 1 \right) \tag{10}$$

http://dx.doi.org/10.5772/52613

4. Measurement methods for SBPL

The plot of eq 10 is presented in Fig. 3. Given data, the SBPL can be obtained by eq 11.

$$l_{sp} = \lim_{L\to\infty} \frac{1}{2}\frac{dD_b}{d\ln L} \tag{11}$$

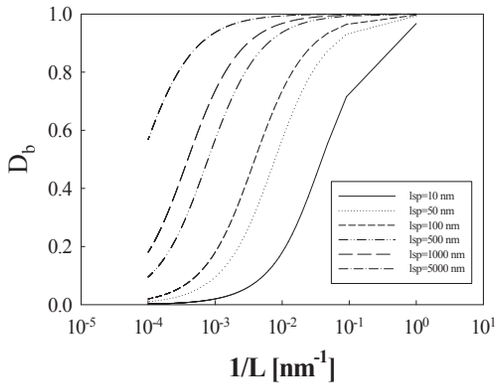

Figure 3. Bending ratio (D_b) with respect to reciprocal contour length.

In this method, one need to have experimental data for $\langle \boldsymbol{R}^2 \rangle$ and L . In order to obtain these data, one have to cut MWCNTs into pieces with various L . Acid cutting or mechanical cutting method may be applied to obtain pieces of MWCNT. It is worth to note that $\langle \boldsymbol{R}^2 \rangle$ are Gaussian, given contour length (L). That is, various end-to-end distances may be measured for a constant L . This method is exact, but hard to obtain the experimental data.

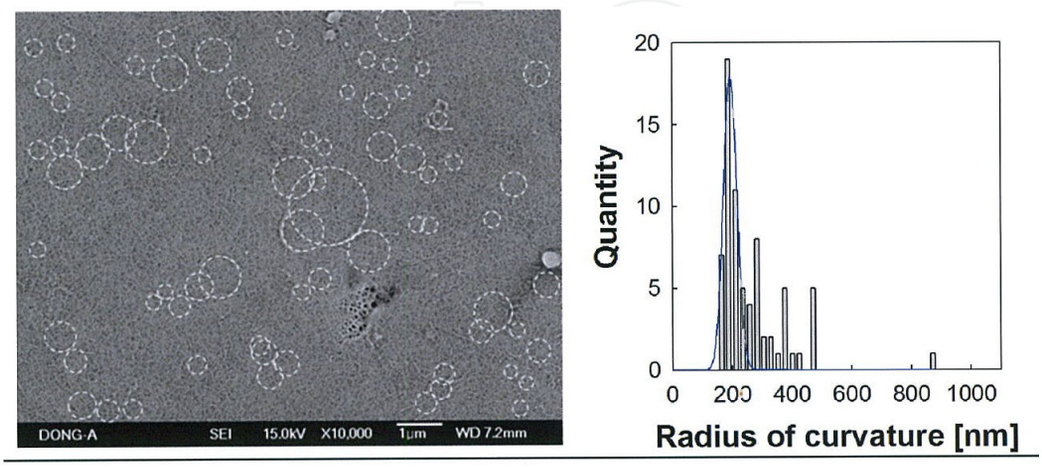

Figure 4. Approximation method to determine SBPL; the mean radius of curvature approximate SBPL.

The mean radius of curvature approximates the SBPL. One can easily obtain the mean value of the radius of curvatures of MWCNTs from any SEM images as seen in Fig. 4. The approximation method is convenient because SEM images of as-synthesized or as-received MWCNT can be directly used. The SBPL obtained by the approximation could have an error up to 200% compared to those obtained by exact method. However, the approximated value of SBPL still has physical significant in many applications, since many applied properties depend on the order of magnitude of SBPL.

5. Intrinsic viscosity of MWCNTs

From the molecular weight, the contour length, and the persistence length, the intrinsic viscosity of MWCNTs can be calculated. If we apply the intrinsic viscosity model of a worm-like coil to the rigid random-coil, the following expressions are obtained,

$$\left[\eta\right] = 2.20x10^{21}\frac{\left\langle R^2\right\rangle^{3/2}}{M}f \tag{12}$$

$$f \cong \left[1 + 0.926\theta\left(D_b\right)^{1/2}\right]^{-1} \tag{13}$$

$$\theta = \ln\left(\frac{2l_{sp}}{e}\right) - 2.431 + \left(e/a\right) \tag{14}$$

where M is molecular weight, $e$is spacing between frictional elements along the contour, $a = \zeta/3\pi\eta_s$, $\zeta$is the friction factor for a single frictional element, and η_s is the solvent viscosity. For the non-draining limit for the random coil, $f = 1$, giving the maximum value of intrinsic viscosity in the model. When we take the static bending persistence length (l_{sp}) as the length of a single frictional element, the friction factor of the element in eq 14 may follow the rigid-rod model such that $\zeta_T = 3\pi\eta_s l_{sp}/\left(\ln\left(l_{sp}/d\right) + 0.3\right)$ for the translational motion and may be $\zeta_r = \pi\eta_s {l_{sp}}^3/\left(3\left(\ln\left(l_{sp}/d\right) - 0.8\right)\right)$ for the end-over-end rotational motion. Translational-rotational coupling and hydrodynamic shielding may also be considered for the evaluation of friction factor in eq 14.In this case, we can surmise that friction factor in eq 14 is scaled with l_{sp}^s, where s is larger than unit value. We can reasonably neglect e/a in eq 14. The measurement of intrinsic viscosity assumes the deformation rate is slow enough. The intrinsic viscosity is determined by the competition of tendency of orientation toward flow direction and tendency to random orientation due to thermal motion (Brownian motion). The measurement often performed at shear rate of several hundreds reciprocal second. At this regime, CNTs may be extended to the static shape by shear force where peclet number

http://dx.doi.org/10.5772/52613

($Pe=\dot{\gamma}(2R_h)^2/D_T$) is over 10.It is worth noting that the static bending persistence length determined from intrinsic viscosity is consistent with that determined from 3-D SEM analysis in dried state.

6. Diffusions of MWCNTs

Not only the toxicological issues but also researches on novel hybrid materials or nano-scale devices points to the need for the understanding of overall shape and mobility of carbon nanotube particles in a solution or in atmosphere.The degree of flexibility of carbon nanotubes is the major ingredient for the shape and mobility, however it is also puzzling.The persistence lengths of single-walled carbon nanotubes are expected to be in the order of tens to hundreds of micrometers due to their exceptionally large modulusand to have longer persistence lengths for muliwalled nanotubes, indicating currently prepared several-micrometer long nanotubes behave like rigid rods. Elastic fluctuations of semi-rigid particles by thermal energy have been described exactly by the worm-like coil model proposed more than 50 years ago by Kratky and Porod. The model describes the stiffness of molecules by dynamic bending persistence lengths (mean radius of curvatures) which are determined by effective bending modulus (E_{eff}) against thermal energy (kT) in a solution. Theoretical calculationshave shown that the dynamic bending persistence lengths (l_ps) of carbon nanotubes (CNTs) are up to several millimetersdue to their exceptionally large Young's modulus of about 1.5 TPa. Real-time visualization technique revealed that l_p s of singlewalled carbon nanotubes (SWCNTs) are between 32 and 174μm, indicating SWCNTs shorter than l_p(=32μm) may be rigid around room temperature in a solution. However, rippling developed on the compressive side of the tube leading to a remarkable reduction of the effective bending modulus, which is more pronounced for multiwalled carbon nanotubes (MWCNTs). Theoretical calculationshave shown that the effective bending moduli of MWCNTs are around 0.5 $nN\ nm^2$ when the radii of curvatures are around 150 ~ 500nm. This indicates MWCNTs longer than 0.5 μmmight be flexible in a solution around room temperature, since thermal energy is about 4.1 x $10^{-3}nN\ nm$. It seems not likely that van der Waals interaction between graphene layers is the only reason that makes the effective bending moduli of MWCNTs more than 100 times smaller than SWCNT.

Both MWCNTs and SWCNTs discussed above are no more than worm-like coils (WLCs) where ensemble average of overall size (end-to-end distance) scales with the square root of molecular weight (contour length) in asymptotic limit. Our recent work has revealed that the spatial average of overall size of MWCNTs also follows the same scaling as WLCs in spite of their static bent points. We designated these MWCNTs as rigid random-coils (RRCs).The only difference between RRCs and WLCs is whether the bending points are static or dynamic by thermal energy.The relationship between the shape and size of RRCs has been characterized by static bending persistence lengths (l_{sp}s). Because both RRCs and WLCs are Gaussian, the models for the mobility of WLCs may also work for RRCs.

Translational diffusion coefficient is defined by the mobility of particle against thermal energy as Einstein relation, eq 15.

$$D = \frac{kT}{\zeta} \tag{15}$$

where k is Boltzman constant, T is temperature, and $1/\zeta$ is the mobility. By analogy to macromolecule, a MWCNT with static bend points can also be considered to be made up N identical structural elements with a frictional factor ζ_e per unit element and a spacing e between elements along the contour of the coil.In this case, the mobility in eq 15 may be expressed as the sum of free-draining contribution $(1/N\zeta_e)$ and hydrodynamic interaction contribution which is called non-draining term.

$$\frac{1}{\zeta} = \frac{1}{N\zeta_e} + \frac{1}{2!N^2}\sum_i\sum_j \frac{1}{\zeta_{ij}} + \cdots \tag{16}$$

where ζ_{ij} is the frictional factor by interaction between ith and jth element and $i \neq j$.

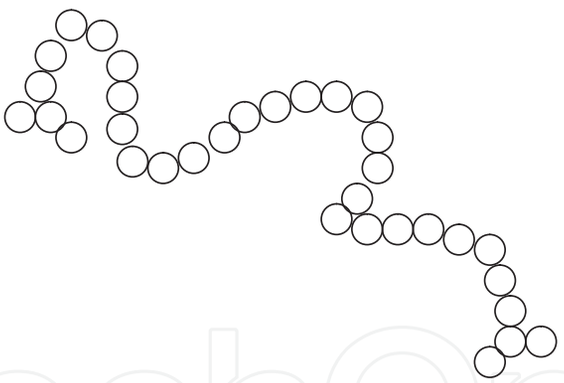

Figure 5. CNT made up N identical frictional element.

When we choose a spherical bead having diameter of a as a frictional element, the frictional factor of each element follows Stokes-Einstein relation, $\zeta_e = 3a\pi\eta_s$ where η_s is the viscosity of solvent. The frictional factor by interaction between ith and jth element may also follow Stokes-Einstein relation since a mean value of distance between elements i and $j$is small. Then, Kirkwood expression is obtained such as eq 17.

$$\frac{1}{\zeta} = \frac{1}{N3a\pi\eta_s}\left[1 + \frac{a}{2Ne}\sum_i\sum_j\left(1-\delta_{ij}\right)\left\langle r_{ij}^{-1}\right\rangle\right] \tag{17}$$

http://dx.doi.org/10.5772/52613

$$\frac{1}{\overline{\overline{R}}_{ij}} = \frac{1}{\overline{\overline{er}}_{ij}} = \left(\frac{1}{e}\right)\sum_i \sum_j \left\langle \left(1-\delta_{ij}\right)\left\langle r_{ij}^{-1}\right\rangle \right\rangle \tag{18}$$

where $r_{ij} \equiv R_{ij}/e$ and R_{ij} is the distance between element i and j,e is solvated diameter of molecule, and N is number of frictional element, $N = L/e$. Here, we can see that mathematical expression for the mobility of RRCs is similar to that of WLCs. Equation 17 is widely used for the estimation of translational diffusion coefficient of macromolecules. Equation 18 has been solved by Hearst and Stockmayer using Riseman-Kirkwood theory and Daniel distribution. We notice that $\bar{r}_{ij}$ is no more than a mean value of distance between the frictional element i and j. Then, $\bar{r}_{ij}$ must depend on the conformation of the carbon nanotubes. Hearst and Stockmayer obtained $\bar{r}_{ij}$ by the Kirkwood-Riseman theory as eq 19.

$$\frac{1}{2}\sum_x \sum_n \left\langle \left(1-\delta_{xn}\right)\left\langle r_n^{-1}\right\rangle_x \right\rangle = \int_1^N dl \int_1^l dn \int_0^\infty F(r,n) r dr = \int_1^N dl \int_1^l dn \int_0^\infty \left[F(r,n) - f(r,n)\right] r dr + \int_1^N dl \int_1^l dn \int_0^\infty f(r,n) r dr \tag{19}$$

where $F(r, n)$ is the unknown distribution for all n, $f(r, n)$ is the known distribution, x is the contour distance of the point of interest from one end of the carbon nanotube, $n$is the contour distance from the point of interest to the frictional element n, and r is the displacement of frictional element n from the point of interest. Hearst and Stockmayer chose the Daniels distribution which includes a first-order correction to a Gaussian distribution as $f(r, n)$, and obtained $\bar{r}_{ij}$ as eq 20.

$$\bar{r}_{ij} = \left[2N\left(\ln\left(2L_p\right) - 2.431 + 1.843\left(N/2L_p\right)^{1/2} + 0.138\left(N/2L_p\right)^{-1/2} - 0.305\left(N/2L_p\right)^{-1}\right)\right]^{-1} \tag{20}$$

where $N = L/e$, L is contour length, $e$is spacing between frictional elements along the contour, $L_p = l_p/e$, and l_p is persistence length. The translational diffusion coefficient of worm-like coil can be estimated by eqs 15, 17, and 20. Rotational diffusion coefficientis expressed as eq 21.

$$D_r = \left(\frac{kT}{\eta_s}\right)\left(\frac{2}{l_p L^2}\right)\left[0.253\left(\frac{L}{4l_p}\right)^{1/2} + 0.159\ln\left(2L_p\right) - 0.387 + 0.160\right] \tag{21}$$

Equations 20 and 21 are valid for a semi-flexible rod when the contour length of rod is much longer than its persistence length such that the mean squared end-to-end distance follows random-coil scaling, $\langle R^2\rangle = N b^2$ where $b = 2l_p$.The semi-flexible rods in this coil limit, $L >> l_p$, are so-called worm-like coils (WLCs). We see that the mobility is determined solely by the

average conformation of particle with a given solvent viscosity and a contour length in eqs 13 and 14. We can reasonably surmise that the diffusion coefficients of RRCs are similar to those of WLCs with a given contour length, if the values of static bending persistence lengths (l_{sp}s) of RRCs are the same as those of the dynamic bending persistence lengths (l_ps) of WLCs.When hydrodynamic shielding effect is taken into account, the diffusion coefficients of RRCs might be slightly larger than those of WLCs due to the static bent points. The root mean-squared end-to-end distance of RRCs are given by eq 22.

$$\left\langle \mathbf{R^2} \right\rangle = \left(N^2 b^2\right)\left(\sum_{i=1}^{k} \varphi_i^2\right)\left(\frac{1+\cos(\theta)}{1-\cos(\theta)}\right) = L^2 D_b \tag{22}$$

$$D_b \equiv \frac{\left\langle \mathbf{R}^2 \right\rangle}{L^2} \cong \left(\sum_{i=1}^{k} \varphi_i^2\right)\left(\frac{1+\cos(\theta)}{1-\cos(\theta)}\right) \cong \left(\frac{2l_{p0}}{L}\right)\left(\frac{1+\cos(\theta)}{1-\cos(\theta)}\right) = C\left(\frac{2l_{p0}}{L}\right) = \frac{2l_{sp}}{L} \tag{23}$$

where D_b is bending ratio, l_{sp} is static bending persistence length, l_{p0} is an arbitrary constant segment length, $\theta$is static bent angle from the MWCNT axis, $\varphi_i = N_i / N$, $N_i$is the number of unit segment in i-direction segment, N is the total number of unit segment, $k = m + 1$, m is the number of static bending points on a coil. When RRCs have semi-flexibility by thermal energy, the ensemble average of bent angle (θ_2) always becomes larger in amount of $\Delta\theta$ than the static bent angle θ;$\theta_2 = \theta + \Delta\theta$. This is due to the fact that the effective bending modulus toward the bent direction is smaller than that toward the opposite direction.This indicates that the overall size of RRCs may be decreased when they are fluctuated by thermal energy. Because frictional elements of RRCs have Gaussian distribution by the definition of RRCs, those of semi-flexible RRCs also have Gaussian distrbution. Therefore, eqs 20 and 21 are also valid for semi-flexible RRCs when the persistence length is replaced by an apparent persistence length. The apparent persistence length (l_{ap}) is determined by the static bent angle (θ) and dynamic bent angle due to thermal energy ($\Delta\theta$) as following.

$$l_{ap} = l_{sp}\left(\frac{1+\cos(\theta+\Delta\theta)}{1-\cos(\theta+\Delta\theta)}\right)\left(\frac{1-\cos(\theta)}{1+\cos(\theta)}\right) \tag{24}$$

Expression for the translational diffusion coefficient of RRCs can be obtained from eqs 15, 17,18, and 24.

$$D_T = \frac{kT}{3\pi\eta_s L}\left[1 + \ln\left(2L_{ap}\right) - 2.431 + 1.843\left(N/2L_{ap}\right)^{1/2} + 0.138\left(N/2L_{ap}\right)^{-1/2} - 0.305\left(N/2L_{ap}\right)^{-1}\right] \tag{25}$$

http://dx.doi.org/10.5772/52613

Similary, expression for the rotational diffusion coefficient of RRCs can be obtained as following.

$$D_r = \left(\frac{kT}{\eta_s}\right)\left(\frac{2}{l_{ap}L^2}\right)\left[0.253\left(\frac{L}{4l_{ap}}\right)^{1/2} + 0.159\ln\left(2L_{ap}\right) - 0.387 + 0.160\right] \tag{26}$$

where $L_{ap} = l_{ap}/e$.Equations 25 and 26 are promising for the estimation of diffusion coefficients of MWCNTs synthesized by a CVD method. In other words, eqs 25 and 26 give us the information of the shape and size of MWCNTs if we have the measured values of diffusion coefficients.

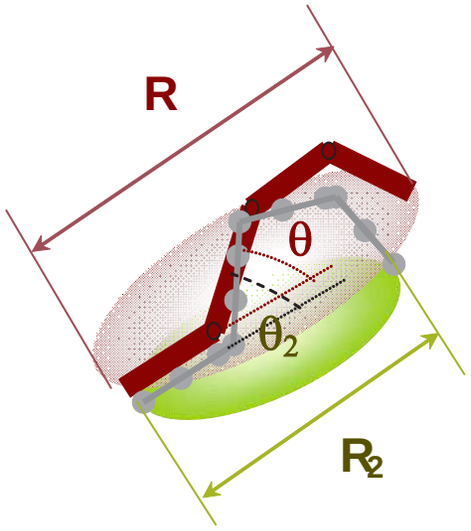

Figure 6. Size of carbon nanotube (R) is decreased to R2 at the elevated temperature.

7. Dynamic light scattering

The translational and rotational Brownian motions lead to fluctuation in the intensity of scattered light.The velocity of particles in Brownian motion can be directly measured by using dynamic light scattering (DLS) method, since time is correlated to obtain the intensity autocorrelation function ($g^{(2)}(t)$). The intensity autocorrelation function is connected to the electric field autocorrelation function ($g^{(1)}(t)$) which is given by eq 27 for a monodisperse solution.

$$\left|g^{(1)}(t)\right| = \exp(-\Gamma t) \tag{27}$$

$$\int_0^\infty G(\Gamma)d\Gamma = 1$$

where $\Gamma = Dq^2$ with D, the translational diffusion coefficient of the molecules, and q, the scattering vector magnitude ($q = 4\pi n \sin(\theta/2)/\lambda_0$ where n is the solution refractive index, θ is the scattering angle, and λ_0 is the incident light wavelength *in vacuo*). For polydisperse solutions, the electric field correlation function is given by a sum or distribution of exponentials,

$$\left|g^{(1)}(t)\right| = \int_0^\infty G(\Gamma)\exp(-\Gamma t)d\Gamma \tag{28}$$

where

In many cases, a single exponent obtained from an average translational diffusion coefficient value fits the decay rate of the electric field correlation function such as eq 29

$$K_1 = \langle\Gamma\rangle_{av} = \int_0^\infty \Gamma G(\Gamma)d\Gamma \tag{29}$$

where K_1 is the first cumulant. When a solution is dilute enough neglecting the interaction between particles, the effective diffusion coefficient can be obtained by the intensity average. The intensity of light scattered by macromolecule species i is often proportional to the molecular weight (M_i) times the weight concentration (c_i). In this case, the intensity average diffusion coefficient equals to z average diffusion coefficient.

The average decay rate (Γ) of the electric field autocorrelation function can be obtained by using conventional DLS.The first cumulant generally fits the data well for carbon nanotube solutions. When the incident light and detector are both vertical, V_v, translational diffusion are characterized by eq 30.

$$\Gamma_{Vv} = q^2 D_T \tag{30}$$

When the incident light vertical and detector horizontal, H_v , the diffusion of anisotropic particle are characterized by eq 31

$$\Gamma_{Hv} = q^2 D_T + 6D_R \tag{31}$$

where D_T is translational diffusion coefficient and D_R is rotational diffusion coefficient. This equation is valid if the particle rotates many times while diffusing a distance comparable to q^{-1} or if there is little anisotropy in particle dimension. MWCNTs solution meets with the former case in this work. Now we have three independent mathematical model eqs 25, 26,

http://dx.doi.org/10.5772/52613

and 12. And two equations for DLS measurement.Three unknown shape factors of static bending persistence length, contour length, and thermal fluctuation angle can be determined from the measured diffusion coefficients and intrinsic viscosity using eqs 25, 26, and 12.This is uniqueness of carbon nanotubes compared to macromolecules, since macromolecules have only two unknown shape factors of persistence length and contour length.

8. Micro rheology

The terminology of "microrheology" is used, to distinguish the technique from conventional (macro) rheology. In the microrheology, colloidal particles are used for probing the rheology of material of interest. The starting point is the Stokes-Einstein relation.

$$D_T = \frac{kT}{6a\pi\eta_s} \tag{32}$$

If we have measured values of translational diffusion coefficient, the viscosity of material of interest can be easily obtained by

$$\eta_s = \frac{kT}{6a\pi D_T} \tag{33}$$

where a is the radius of spherical colloidal particle; colloidal particles have usually average diameter between 1 nm and 1000 nm. It is comparable the ISO definition of nanoparticles those have average diameter between 1 nm and 100 nm. In this sense, nanoparticles are just some kinds of colloidal particles. When we have measured value of mean-squared displacement of probe particle, the following equation can be utilized.

$$\left\langle r^2(t) \right\rangle = 6D_T t = \frac{kT}{\pi a \eta_s} \tag{34}$$

This seemingly simple idea has done a great impact on various research fields, indeed. One example is the nanoparticles dispersed in a polymer melt. It is often reported that nanoparticles seems diffuse faster than expected. The origin of this phenomenon lies in the "Nano" size. The viscosity of polymer melt is well described by integral constitutive equations such as reptation model. In this model, the viscosity is determined by the stress relaxation time of polymer chain from the constraint of entanglement. When the observation time is much shorter than any relaxation time of polymer in rheometry of frequency sweep, the polymers behave like a crosslinked rubber, exhibiting a plateau modulus. The plateau modulus of polymers is determined from the entanglement lengths of polymer such as

$$G_o^N = \frac{\rho RT}{M_e} \tag{35}$$

The plateau modulus of polymer is usually reported in the order of $10^{6\sim7}$Pa. Entanglement molecular weight of polymer is about 1000~2000 g/mole. The entanglement length is about 10~100 nm.The particles having comparable size to the entanglement length of a polymer would feel less frictional force than expected from the melt viscosity in macrorheology. Therefore, viscosity of polymer melt is much lower for the nanoparticles. This may lead to the faster thermal motion of nanoparticle compared to a larger particles.

9. Applications

In our previous works, we demonstrated that MWCNT having shorter SBPL have a certain merit in a polymer composite for electrical conductive application. When MWCNTs are needle-like, polymer composites comprised of them exhibit higher electrical conductivity compared to those comprised of tortuous MWCNTs. The situation changed drastically when the composites were molded into a specimen by injection molding machine. The needle like CNTs aligned to the flow direction, which broke the electrical conductive networks, then the composites lose the electrical conductivity. However, this problem was not observed when the composites contained tortuous MWCNTs which have a short SBPL. We also showed that the electrical percolation threshold depends on the length of MWCNT when MWCNT are needle-like. But, the electrical percolation threshold depends on the SBPL for a tortuous MWCNT. Thermal conductivity and linear thermal expansivity are also strongly dependant properties on the SBPL of MWCNT. Especially, thermal shrinkable material can be fabricated as well as thermal expansive material by controlling SBPL of MWCNT.

Author details

Heon Sang Lee

Address all correspondence to: heonlee@dau.ac.kr

Dong-A University, Department of Chemical Engineering, Sahagu, Busan, South Korea

References

[1] Lee, H. S.; Yun, C. H.; Kim, S. K.; Choi, J. H.; Lee, C. J.; Jin, H. J.; Lee, H.; Park, S. J.; Park, M. Appl. Phys. Lett. 2009, 95, 134104.

[2] Lee, H. S.; Yun, C. H. J. Phys. Chem. C 2008, 112, 10653-10658.

[3] Lee, H. S.; Yun, C. H.; Kim, H. M.; Lee, C. J. J. Phys. Chem. C 2007, 111, 18882- 18887.

[4] Han, M. S.; Lee, Y. K.; Yun, C. H.; Lee, H. S.; Lee, C. J.; Kim, W. N. Synthetic Metals 2011, 161, 1629-1634.

[5] Heo, Y. J.; Yun, C. H.; Kim, W. N.; Lee, H. S. Curr. Appl. Phys. 2011, 11, 1144-1148.

[6] Hearst, J. E.; Stockmayer, W. H. J. Chem. Phys. 1962, 37, 1425-1433.

[7] Squires, T. M.; Mason, T. G. Ann. Rev. Fluid Mech. 2010, 42, 413-438.

[8] Hearst, J. E. J. Chem. Phys. 1963, 38, 1062-1065.

[9] Hearst, J. E. J. Chem. Phys. 1964, 40, 1506-1509.

[10] Kratky, O; Porod, G. Recl. Trav. Chim. Pays-Bas 1949, 68, 1106-1122.

[11] Doi, M.; Edwards, S. F. The theory of polymer dynamics; Oxford University Press: New York, U.S., 1986.

[12] Berne, B. &Pecora, R. Dynamic Light Scattering; Wiley: New York, 1976.

[13] Tanford, C. Physical Chemistry of Macromolecules; John Wiley & Sons: New York, 1961.

[14] Koppel, D. E. J. Chem. Phys. 1972, 57, 4814-4820.

[15] Cush, R.; Russo, P. S.; Kucukyavuz, Z.; Bu, Z.; Neau, D.; Shih, D.; Kucukyavuz, S.; Ricks, H. Macromolecules1997, 30, 4920-4926.

IntechOpen